

AGS LOW FIELD CORRECTION ELEMENTS\*

J.C. Herrera, C. Lasky, and M. Month  
Brookhaven National Laboratory  
Upton, New York

I. Introduction

The Brookhaven Alternating Gradient Synchrotron accelerates protons from an injection energy of 50 MeV to a final energy of 30 GeV. During the initial phase of the process, the motion of the particles is determined primarily by the injection fields and their gradients existing along the half mile circumference of the machine. It is our purpose to consider the effects of linear magnetic components on the motion of these low energy protons. In Sections II and III we will treat superperiod-quadrupoles (Fig. 1) and dipole elements in some detail. In addition, we include in Table 1 a summary of the characteristics of other linear components.

II. Quadrupoles and Betatron Motion

A particle moving stably in an alternating gradient synchrotron describes a motion about an equilibrium orbit satisfying the equation<sup>1</sup>

$$y(s) = W^{\frac{1}{2}} \beta^{\frac{1}{2}}(s) \cos [\nu\varphi(s) + \delta] \quad (1)$$

where

$y(s)$  = the horizontal or vertical displacement,  
 $s$  = the distance along the equilibrium orbit,  
 $\beta(s)$  = the periodic amplitude function,

$\nu = \frac{1}{2\pi} \int_0^C \frac{d\rho}{\beta(\rho)}$ , the number of betatron oscillations per revolution,

$\nu\varphi(s) = \int_0^s \frac{d\rho}{\beta(\rho)}$ , the betatron phase [ $\varphi(s)$  is approximately equal to the physical angle at any point along the circumference of the ring],

$W, \delta$  = parameters determined by the initial conditions.

Insofar as the motion is characterized by this equation, it is only the two amplitude functions,  $\beta_H$  and  $\beta_V$ , which determine the particle behavior. In practice,<sup>1</sup> the two quantities  $\nu$  and the maximum value of the amplitude function,  $\beta_{max}$ , are used as basic machine parameters. The former ( $\nu$ ) serves as an indicator of the stability of the motion ( $\nu$  integer or half-integer associated with instability), while the latter ( $\beta_{max}$ ) is a measure of the machine phase space admittance ( $A \propto 1/\beta_{max}$ ).

In the present AGS there are quadrupoles (Fig. 2, Table 2) in each of the 3 (position of a maximum in  $\beta_V$ ) and 17 (position of a maximum in  $\beta_H$ ) straight sections of the twelve superperiods

of the ring. Their primary use is to provide control of the  $\nu$  values, vertical and horizontal, between 8 and 9. Figure 3 shows<sup>2</sup> a plot of the changes in  $\nu_H$  and  $\nu_V$  that can be obtained for different quadrupole integrated field strengths (G). A typical operating point is with  $G(3)$  equal to 100 gauss and  $G(17)$  equal to 200 gauss. These added gradient fields, as can be seen from the figure, have the effect of lowering the horizontal and raising the vertical  $\nu$  values ( $\nu_H \approx 8.2$ ,  $\nu_V \approx 8.9$ ). Such a mode of operation changes the  $\beta$  function as shown in Fig. 4. The important point illustrated here is that the vertical beta function determining the vertical admittance (which because of the smaller vertical aperture is less than the horizontal admittance) has not been increased by more than about 5% at any point over the entire ring.

In the preceding paragraph we have pointed out that the main function of the superperiod quadrupoles is to shift the  $\nu$  values. Another possible application of a quadrupole distribution over the superperiod is that of correcting the  $\beta$  function; that is, adding gradient to the machine in order to obtain an amplitude function that does not have one maximum larger than another. That this is an optimum condition as far as admittance is concerned can be seen from the fact that it is the largest maximum that determines the admittance. Figure 5 for the horizontal and Fig. 6 for the vertical motion include curves (solid lines) for the amplitude function over one superperiod for the machine with the main ring magnets (no quads) at injection field. A large difference in the maxima of the beta functions is evident, with the largest occurring at straight section 5 for  $\beta_H$  and at straight section 15 for  $\beta_V$ . To eliminate this  $\beta_{max}$  variation (physically arising because of the difference in the remanent gradient in the open and closed magnets of the AGS<sup>3</sup>), quadrupoles can be placed at the even straight sections 2, 8, 12, and 18. Using in our calculation the strengths and polarities indicated in Figs. 5 and 6, we obtain both vertical and horizontal beta functions having the desired uniformity in their maxima (dashed lines). The specific nature of the corrections introduced by this arrangement of quadrupoles is best seen by considering the fractional change of the beta function. Thus in Fig. 7 as well as Fig. 8 we see a single cycle of  $\Delta\beta/\beta$  which, over the 12 superperiods, is equivalent to a 12<sup>th</sup> harmonic correction. Since the average change in  $\Delta\beta/\beta$  is small, the accompanying  $\nu$  change is correspondingly small ( $\Delta\nu_H, \Delta\nu_V \approx 0.05$ ). In order to shift the  $\nu$  values without upsetting the above corrections to the amplitude function, additional gradient changes must be distributed evenly (located at  $\beta_{max}$  and  $\beta_{min}$  positions) over the superperiod. Detailed calculations on this aspect of the problem have yet to be performed.

\*Work performed under the auspices of the U.S. Atomic Energy Commission.

### III. Dipole Fields and Equilibrium Orbit Displacement

In this section we describe the dipole corrections now in the AGS. These provide a control over the shape of the equilibrium orbit. At present there are only vertical correction coils, although horizontal ones are being considered. The theory for calculating the effect produced on the particle motion by such a dipole field distribution is given in Courant and Snyder.<sup>1</sup> The general result for a number (N) of point dipoles distributed around the circumference of the ring may be written as a Fourier series:

$$y_{E.O.}(s) = \frac{\beta^{\frac{1}{2}}(s)}{2\pi\nu(H\rho)} \left[ \sum_{j=1}^N [\Delta B_r(j)\ell] \beta^{\frac{1}{2}}(s_j) + \sum_{n=1}^{\infty} \left\{ \frac{2\nu^2}{\nu^2 - n^2} \sum_{j=1}^N [\Delta B_r(j)\ell] \beta^{\frac{1}{2}}(s_j) \cos(n\varphi(s_j)) \right\} \cos n\varphi(s) + \sum_{n=1}^{\infty} \left\{ \frac{2\nu^2}{\nu^2 - n^2} \sum_{j=1}^N [\Delta B_r(j)\ell] \beta^{\frac{1}{2}}(s_j) \sin(n\varphi(s_j)) \right\} \sin n\varphi(s) \right] \quad (2)$$

where

- $y_{E.O.}(s)$  = displacement of the equilibrium orbit at point  $s$  along the central reference orbit,  
 $H\rho$  = magnetic rigidity of the particle,  
 $\Delta B_r(j)\ell$  = integrated field strength at the point  $s_j$ ,  
 $n$  = harmonic number,

and  $\nu$ ,  $\beta(s)$ ,  $\varphi(s)$  are as given following Eq. (1).

The dipole coils whose characteristics appear in Table 3, are positioned and powered as shown in Figs. 9 and 10. They predominantly produce 8<sup>th</sup>, 9<sup>th</sup>, and 12<sup>th</sup> harmonic field distributions around the circumference of the machine. Physically, the 12<sup>th</sup> harmonic coils (120) are used for cancelling the effect of the earth's field which, because of the arrangement of the ring magnets in the super-period structure (see Fig. 1: the first 10 magnets have their back legs on the outside of the ring while the last 10 have them on the inside), produce a 12<sup>th</sup> harmonic vertical displacement in the equilibrium orbit. On the other hand, the 80 and 90 coils are used to correct for perturbing horizontal fields which could yield a large distortion due to the resonant denominator in Eq. (2) ( $\nu = 8.9$ ). In Table 4 we give the contribution to the equilibrium orbit displacement obtainable from each of the above sets of coils. These have been calculated from Eq. (2) using the  $\beta(s)$  and  $\varphi(s)$  functions computed by the BEAM program.

#### Acknowledgements

We would like to thank Dr. A. Maschke and Dr. M. Barton for helpful suggestions and discussions.

#### References and Footnotes

1. E.D. Courant and H.S. Snyder, Ann. of Phys. 3, 1 (1958).
2.  $\nu$  values and  $\beta$  functions are obtained using the computer program BEAM. The  $\nu$  value shift of Fig. 3 as well as the first order perturbation theory curves of  $\Delta\beta/\beta$  in Figs. 4, 7, and 8 are calculated from the results given in BNL Accelerator Department Internal Report AGSCD-14.
3. R.A. Beth and C. Lasky, Science 128, 1393 (1958).

Table 1

Low Field Correction Elements for the BNL AGS

	Element	Superperiod Symmetry	Location	Horizontal (H) and/or Vertical (V) Function	Effect on Particle Motion	
Gradient	Superperiod Quadrupoles	Yes	Straight Sections 3 and 17	HV	Provides $\nu$ value control. $\nu_H$ and $\nu_V$ (8.2 and 8.9) separation prevents transfer from horizontal to vertical motion.	
	(17 $\theta$ ) Quads	No	Straight Section 17 in Superperiods C, F, I, & L	H	Corrects for the horizontal gradient stopband at $\nu = 8^{1/2}$ .	
Field	12 $\theta$ sin 12 $\theta$	Yes	Fig. 10	V	Corrects the 12 <sup>th</sup> harmonic vertical distortion of the equilibrium orbit produced by the earth's magnetic field.	
	9 $\theta$	sin 9 $\theta$	No	Fig. 9	V	Corrects for the 8 <sup>th</sup> and 9 <sup>th</sup> harmonic vertical distortion in the equilibrium orbit due to perturbing fields
		cos 9 $\theta$				
	8 $\theta$	sin 8 $\theta$				
cos 8 $\theta$						
Gradient Coupling	"Twist Quad" Field	No	8 $\theta$ & 9 $\theta$ Coils Fig. 9	HV	Operation of the 8 <sup>th</sup> and 9 <sup>th</sup> harmonic coils with opposing currents produces a tilted quadrupole field component (bucking field). This corrects for the horizontal to vertical coupling due principally to the earth's magnetic field.	
	(17 $\theta$ ) Skew Quads	No	B-15, E-15 H-15, K-15	HV	Corrects for the coupling gradient stopband at $\nu_H + \nu_V = 17$ .	

Table 2

Quadrupoles in Straight Sections 3 and 17

Half Aperture	- 3" = 7.62 cm
Turns/Pole	- 16
Length, Actual	- 24" = 61 cm
Length, Effective	- 68 cm
Gradient	- 0.694 x amps (gauss/cm)
$\int G d \ell$	- 47 x amps (gauss)

Table 3

8 $\theta$ , 9 $\theta$ , and 12 $\theta$  Correcting Coils

Turns	- 160 each coil
Copper size	- 0.010" x 0.50"
Length, Mean Turn	- 31.6" = 80 cm
I.D.	- 4.12" x 7.25"
R	- 0.67 ohms/coil
Coil Separation	- 12" approx.
$\int B d \ell$	- 49 gauss-cm/amp (2 coils)

Table 4

Harmonic Field Corrections in the AGS

Designation	$\nu_y$	$y_{E,0.}(s)$ , inches	$y_{E,0.}(s)$ , inches	I, amps	y for I amps
sin 12 $\theta$	8.757	$y(s) = -\beta^{\frac{1}{2}}(s)(0.0034 I) \sin 12\varphi$	$y = \frac{\beta^{\frac{1}{2}}(s)}{\beta_{avg}^{\frac{1}{2}}} (-0.081 I) \sin 12\varphi$	2	$y = \frac{\beta^{\frac{1}{2}}(s)}{\beta_{avg}^{\frac{1}{2}}} (-0.16) \sin 12\varphi (s)$
sin 9 $\theta$	8.898	$y(s) = -\beta^{\frac{1}{2}}(s)(0.039 I) \sin 9\varphi$	$y = \frac{\beta^{\frac{1}{2}}(s)}{\beta_{avg}^{\frac{1}{2}}} (-0.94 I) \sin 9\varphi$	0.15	$y = \frac{\beta^{\frac{1}{2}}(s)}{\beta_{avg}^{\frac{1}{2}}} (-0.14) \cos 9\varphi (s)$
cos 9 $\theta$	8.898	$y(s) = -\beta^{\frac{1}{2}}(s)(0.039 I) \sin 9\varphi$	$y = \frac{\beta^{\frac{1}{2}}(s)}{\beta_{avg}^{\frac{1}{2}}} (-0.94 I) \cos 9\varphi$	0	$y = 0$
sin 8 $\theta$	8.898	$y(s) = \beta^{\frac{1}{2}}(s)(0.0031 I) \sin 8\varphi$	$y = \frac{\beta^{\frac{1}{2}}(s)}{\beta_{avg}^{\frac{1}{2}}} (0.073 I) \sin 8\varphi$	0.45	$y = \frac{\beta^{\frac{1}{2}}(s)}{\beta_{avg}^{\frac{1}{2}}} (0.033) \sin 8\varphi (s)$
cos 8 $\theta$	8.898	$y(s) = \beta^{\frac{1}{2}}(s)(0.0034 I) \cos 8\varphi$	$y = \frac{\beta^{\frac{1}{2}}(s)}{\beta_{avg}^{\frac{1}{2}}} (0.081 I) \cos 8\varphi$	0.9	$y = \frac{\beta^{\frac{1}{2}}(s)}{\beta_{avg}^{\frac{1}{2}}} (0.073) \cos 8\varphi (s)$

$R = 5055 \text{ inches} \quad , \quad \beta_{avg} = \frac{R}{\nu}$

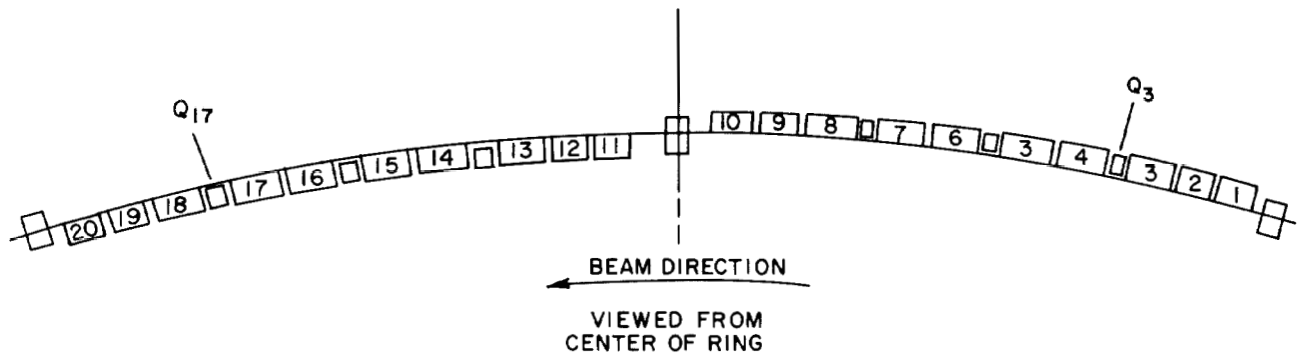


Fig. 1. Typical superperiod—straight section number corresponds to that of upstream magnet.

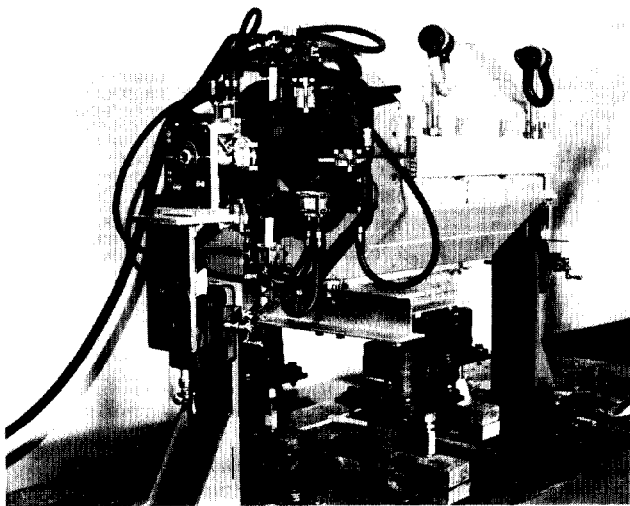


Fig. 2. Photograph of G(3) and G(17) ring quadrupole.

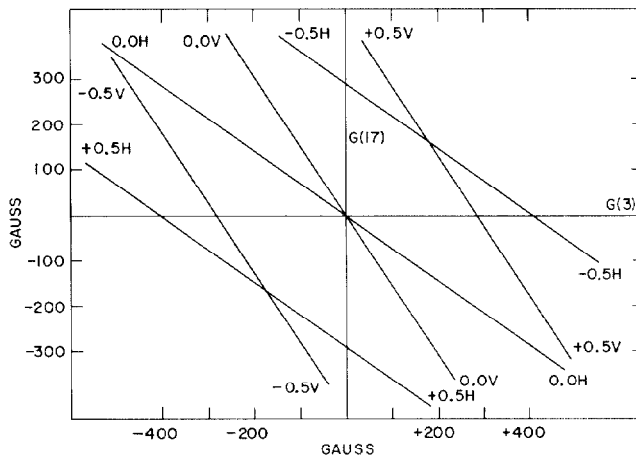


Fig. 3. First order change in  $\beta$  for quadrupoles in straight sections 3 and 17.

$G(3)$  and  $G(7)$  = gradient  $\times$  length = gauss  
 $P = 4.114 \times 10^5$  gauss-in.  
 $(\nu_H)_0 = 8.6153$   
 $(\nu_V)_0 = 8.4923$  } computed from BEAM  
 $\Delta \nu_H = -G(3) (0.00123338) - G(17) (0.00171734)$   
 $\Delta \nu_V = G(3) (0.00176652) + G(17) (0.00114834)$

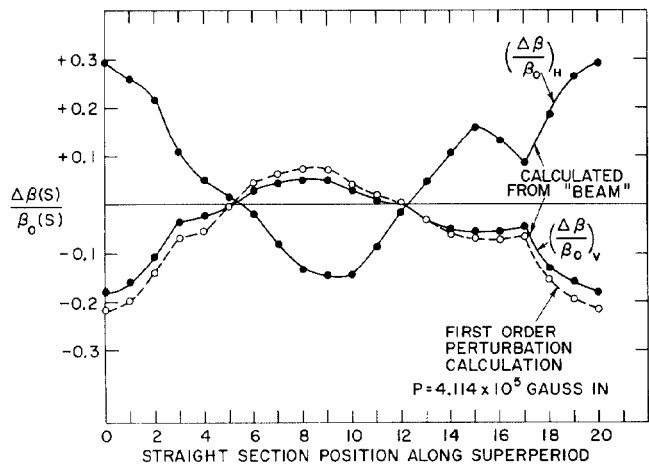


Fig. 4. Fractional change in vertical and horizontal amplitude function with quadrupoles in straight sections 3 and 17.

Straight Section	3	17
Vertical Effect	F	F
Horizontal Effect	D	D
Integrated Strength (gauss)	100	200

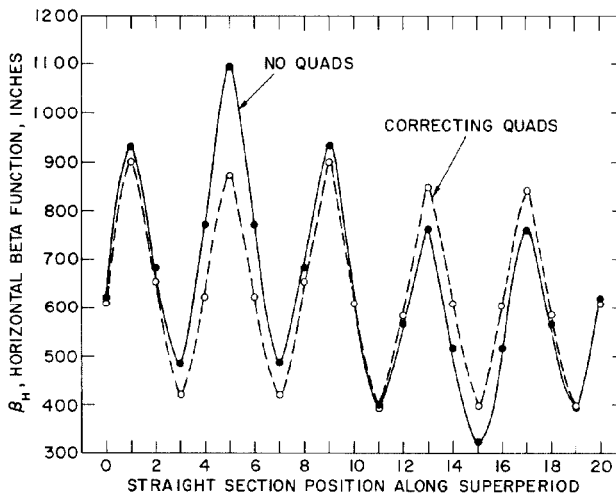


Fig. 5. Horizontal amplitude function ( $\beta_H$ ) correction with quadrupoles in straight sections 2, 8, 12, 18.

Straight Section	2	8	12	18
Focussing or Defocussing	F	F	D	D
Integrated Strength (gauss)	120	120	-120	-120

$\bullet \nu_H = 8.6851$   
 $\circ \nu_V = 8.7390$  } computed from BEAM

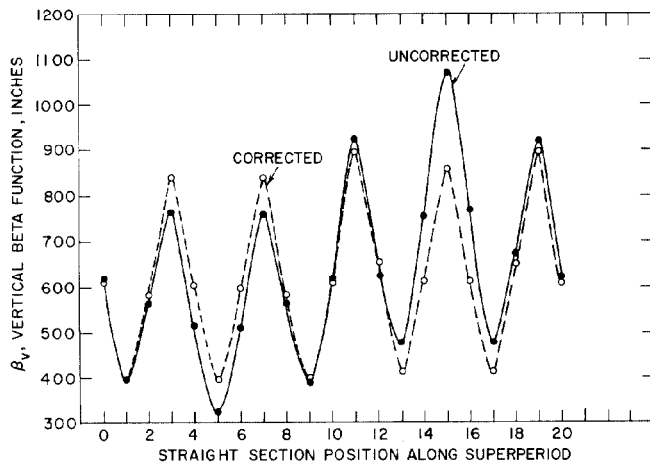


Fig. 6. Vertical amplitude function ( $\beta_V$ ) correction with quadrupoles in straight sections 2, 8, 12, 18.

Straight Section	2	8	12	18
Focussing or Defocussing	D	D	F	F
Integrated Strength (gauss)	-120	-120	120	120

$\bullet \nu_V = 8.7573$   
 $\circ \nu_V = 8.8079$       computed from BEAM

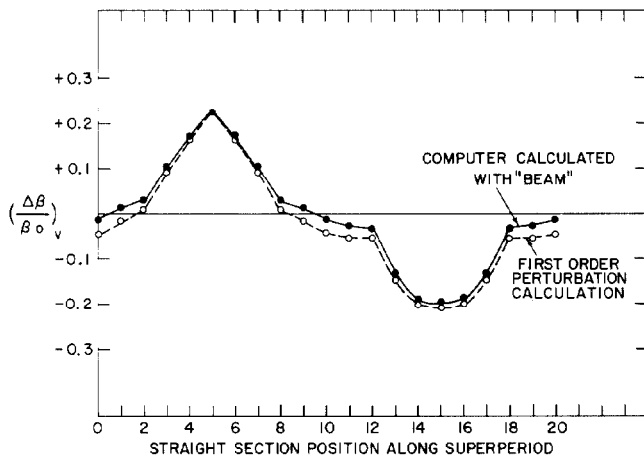


Fig. 8. Fractional change in vertical amplitude function with correction quadrupoles as in Fig. 6.

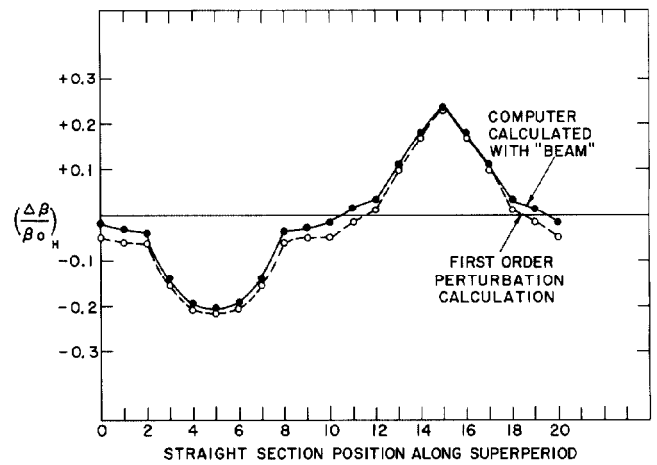


Fig. 7. Fractional change in horizontal amplitude function with correction quadrupoles as in Fig. 5.

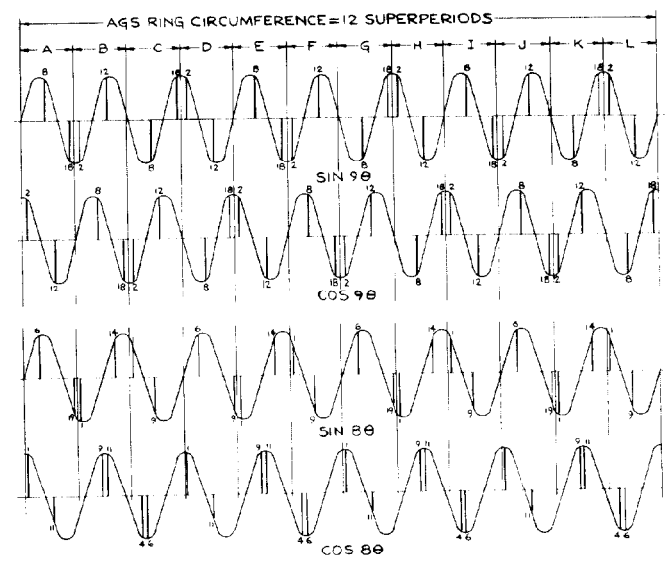


Fig. 9. Physical locations and polarities of  $8\theta$  and  $9\theta$  correction coils.

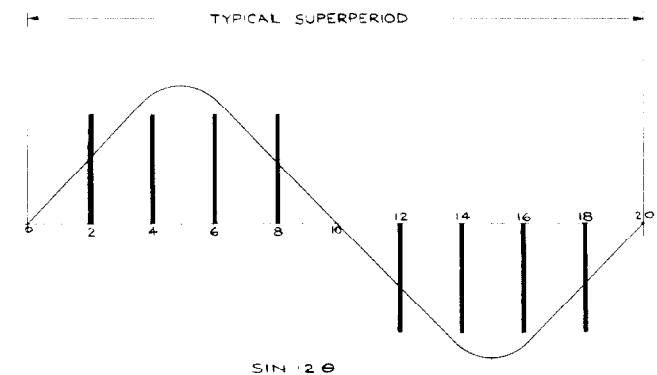


Fig. 10. Physical locations and polarities of  $12\theta$  correction coils.